Journal of Non-Crystalline Solids 274 (2000) 208–231

www.elsevier.com/locate/jnoncrysol

Section 15. Phase transformation kinetics I

Surface crystallization of silicate glasses: nucleation sites and kinetics

R. Müller [a], E.D. Zanotto [b,*], V.M. Fokin [c]

[a] *Federal Institute for Materials Research and Testing, Branch Adlershof, Rudower Chaussee 5, D-12489 Berlin, Germany*

[b] *Vitreous Materials Laboratory – LaMaV, Department of Materials Engineering, Federal University of São Carlos – Ufscar, P.O. Box 676, 13565-905, São Carlos, SP, Brazil*

[c] *Grebenshchkov Institute of Silicate Chemistry, St. Petersburg, Russian Federation*

Abstract

In this paper we review some pertinent research aimed at understanding surface nucleation from both qualitative and quantitative points of view. The majority of quantitative studies discuss the crystal nucleation kinetics of soda-lime-silica glasses and alkali-free silicate (cordierite, anorthite and diopside) glasses. We emphasize the kinetics of surface nucleation and consider the effects of surface quality, tips, cracks and scratches, foreign particles and surrounding atmosphere on crystallization. Related nucleation mechanisms are discussed.

1. Introduction

Devitrification starts most readily from glass surfaces if volume nucleation is not promoted by nucleating agents, usually employed in the manufacture of conventional glass-ceramics (e.g. [1]). Surface crystallization is often related to the undesired devitrification of glass articles during fabrication or to the manufacture of some types of glass-ceramics via sintering and crystallization of glass powders. Measured against its scientific and technological importance, the mechanisms and kinetics of surface nucleation have drawn little attention and are not well understood so far.

Against that background, the Technical Committee 7 (TC-7) of the International Commission on Glass started a cooperative program to advance the understanding of surface nucleation and crystallization phenomena in 1990. The crystallization of metastable high-quartz solid solution crystals ('μ-cordierite') and 'X-phase' crystals (both of cordierite composition $2MgO–2Al_2O_3–5SiO_2$) in cordierite glass were chosen as model cases. This choice was mainly due to the chemical durability of cordierite glass, its polymorphic course of crystallization [2], and the absence of volume crystallization [3]. Attention was also drawn to the surface crystallization of anorthite ($CaO–Al_2O_3–2SiO_2$) and diopside ($MgO–CaO–2SiO_2$) in their iso-stoichiometric glasses for similar reasons.

Here we review our most relevant results concerning surface nucleation and other literature on this matter. Attention is given to surface nucleation kinetics and the properties of nucleation sites. The potential benefit of this knowledge is described elsewhere [4]. Thus, at least for cordierite glass powders, the number of active sites could be

* Corresponding author. Tel: +55-162 60 8244; fax: +55-162 61 5404.

E-mail address: dedz@power.ufscar.br (E.D. Zanotto).

0022-3093/00/$ - see front matter
PII: S0022-3093(00)00214-3

explained in terms of the hypotheses reviewed in this article and the sinterability of these powders could be successfully controlled [4]. Impressive control of sintering and crystallization kinetics and improvement of thermal properties of sintered cordierite glass-ceramics were attained [5,6].

2. Surface nucleation kinetics

2.1. Theory

2.1.1. Homogeneous nucleation

Basic equations. Nucleation data are most frequently discussed in the framework of the classical nucleation theory, CNT (e.g. [7–9]). Here, a few equations are given on which the discussion of surface nucleation kinetics is based. In terms of the CNT, the steady-state homogeneous nucleation rate, I_0 [1/m^3 s], can be approximated by

$$I_0(T) \approx \frac{kT}{3\pi\lambda_M^3\eta(T)} n_0 \exp\left(-\frac{W(T)}{kT}\right), \tag{1}$$

where W is the work of forming a critical nucleus, T the absolute temperature, and η the viscosity of the melt. λ_M approximates both the jump distances of the molecular building units of the glass forming melt ('monomers') and their size. n_0 is their number per unit volume that depends on the monomer volume $v_M \approx \lambda_M^3 \approx M/\rho_M N_A$, where M is the molar weight of the monomers, ρ_M the density of the melt and N_A the Avogadro's number. For spherical particles, W is given by

$$W(T) = \frac{16\pi V_C^2 \sigma_{CM}^3}{3\Delta\mu(T)^2}, \tag{2}$$

where $V_C = N_A v_C$ is the molar volume of the crystal phase, $v_C \approx \lambda_C^3 \approx M/(\rho_C N_A)$ the monomer volume in the crystal phase, and ρ_C the density of the crystal. $\Delta\mu$ is the molar free enthalpy change of crystallization for one-component systems (thermodynamic driving force of crystallization), which is given for $T < T_M$ by [10]

$$\Delta\mu(T) = -\frac{\Delta H_M}{T_M}(T_M - T) - \int_T^{T_m} \Delta C_p(T')\,dT' + T\int_T^{T_m} \frac{C_p(T')}{T'}\,dT', \tag{3}$$

where $\Delta C_p < 0$ is the crystal-melt difference in specific heats at constant pressure, ΔH_M the *molar* enthalpy of fusion and T_M the melting temperature. $\Delta H_M = \Delta Q \cdot M$ can be obtained from the specific heat of fusion, ΔQ. The crystal–melt interfacial energy, σ_{CM} in Eq. (2), can be approximated by [11]

$$\sigma_{CM} = \alpha\Delta H_M(\rho_c/M)^{2/3} N_A^{-1/3}, \tag{4}$$

where α is an empirical constant. From fitting CNT to the volume nucleation rate data for several silicate glasses, taking M as the formula weight of the crystal, $0.45 < \alpha < 0.56$ [12] was obtained.

The effect of time, t, upon the non-steady-state homogeneous nucleation rate, I, can be approximated by Eq. (5) (e.g. [7,9,13]) with $\tau \approx \sigma_{CM} N_A^2 \eta \lambda_M^5 / Z\Delta\mu^2$, where Z is a dimensionless steric factor between 10^{-2} and 10^{-4} [14].

$$I(t) = I_0 \exp\left(-\frac{\tau}{t}\right). \tag{5}$$

Problems. The application of CNT has several difficulties. Basic assumptions, including the use of shear viscosity to calculate the transport part or the constancy of σ_{CM} are questionable [9]. Furthermore, although I_0 depends on σ_{CM} the latter cannot be measured directly. Thus, assumptions about α and M in Eq. (4) affect I_0. This problem is expressed substituting appropriate expressions for ΔH_M and V_C:

$$\sigma_{CM} \approx \alpha(\lambda_C \rho_C)\Delta Q, \tag{6}$$

where $\lambda_C \rho_C$ is the specific surface area formed by 1 g of the crystal phase if all monomers are arranged in a single layer. α and λ_C are difficult to estimate. Assuming M to be equal to the crystal formula weight, as done in most previous papers (see e.g. [9]), is questionable, at least for framework glasses. Thus, calculations of the expected homogeneous volume nucleation rate of μ-cordierite in cordierite glass [15] have shown that altering α (or λ) by a factor of 2 can alter the nucleation rate by 50 orders of magnitude! Moreover, it has been argued that *metastable* phases might precipitate in the early stages of nucleation of most glasses. Hence, the use of thermodynamic data for the stable phase

in Eq. (3) might produce misleading results for the driving force, $\Delta\mu$ (e.g. [16]).

2.1.2. Homogeneous and heterogeneous internal and surface nucleation

Homogeneous volume nucleation. In this case, the experimentally obtained ('apparent') nucleation rate, dN_V/dt [1/m^3 s], equals I because homogeneous nucleation occurs randomly with equal probability at every point in the liquid:

$$\frac{dN_V}{dt} \equiv I. \tag{7}$$

Heterogeneous volume nucleation. In this case, nucleation starts from nucleation sites dispersed in the glass volume. dN_V/dt is not only a characteristic property of the liquid but depends also on the number density of the sites, S_V [1/m^3], and the nucleation rate at these sites, I_S [1/s], according to Eq. (8).

$$\frac{dN_V}{dt} = S_V I_S. \tag{8}$$

Physical interpretation of I_S can follow two *concepts*. Nucleation can (i) be considered to occur from solid particles with a surface nucleation rate I^+ [1/m^2 s]. Assuming a surface area s^* for each particle, $I_S = s^* I^+$ results. I_0^+, the steady-state $I^+(T)$, can be described in terms of Eq. (1) replacing n_0 by $n_0^{2/3}$ [1/m^2] and W by $W^* = W\Phi$, where $\Phi < 1$ denotes the nucleating activity of the substrate and can be considered as a function of the wetting angle, $\Phi(\theta)$. $I^+(t)$ is described by Eq. (5) replacing I_0 by I_0^+ and τ by $\tau^* \approx \tau\Phi^{1/2}$ [10]. Alternatively, (ii) nucleation can be considered to occur within a small activated volume, v^*, in the vicinity of each nucleation site. $I_S = v^* I^*$ results, where I^* [1/m^3 s] is the volume nucleation rate per unit activated volume. v^* can represent, for example, the vicinity along a surface scratch or the interface layer around solid particles embedded in the melt, as illustrated in Fig. 1(a). The temperature dependence of I_S, given by $I^+(T)$ or $I^*(T)$, deviates from $I(T)$. If the nucleation activity within v^* is solely described by Φ, $I^*(T)$ is increased by reducing W^* as in the case of $I^+(T)$. This effect is illustrated in Fig. 2. Because the impact of W on I is most effective for small undercoolings, I increases at high temperatures. For $T <\approx T_g$, I is limited by η and a smaller change of I results. However, within v^*, all CNT parameters (such as σ_{CM} or η) may alter, causing a local

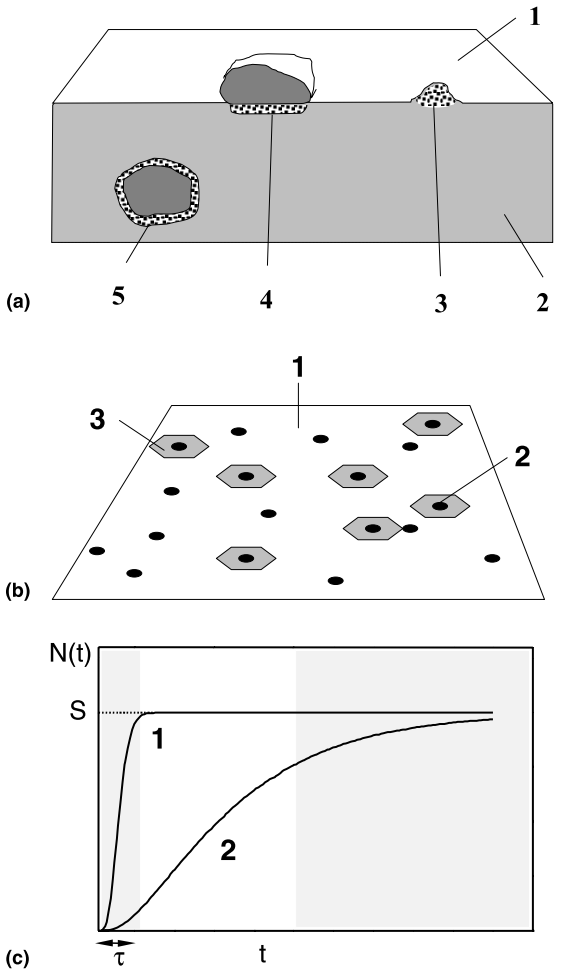

Fig. 1. (a) Schematic representation of local 'activated' volumes, v^*, where enhanced nucleation could occur due to the altered glass properties. 1: glass surface, 2: glass volume, 3: v^* at a surface tip, 4: v^* in the vicinity of a solid particle placed at the glass surface, 5: v^* around a solid particle embedded in the melt. (b) Schematic representation of the 'using-up' of surface nucleation sites. 1: glass surface, 2: randomly distributed surface nucleation sites, 3: surface crystals. (c) Schematic surface nucleation kinetics. 1: $N(t)$ for a high value of I_S, 2: $N(t)$ for a low value of I_S. The shadowed regions indicate experimental limits related to the minimum size of detectable crystals (left) and to crystal impingement (right).

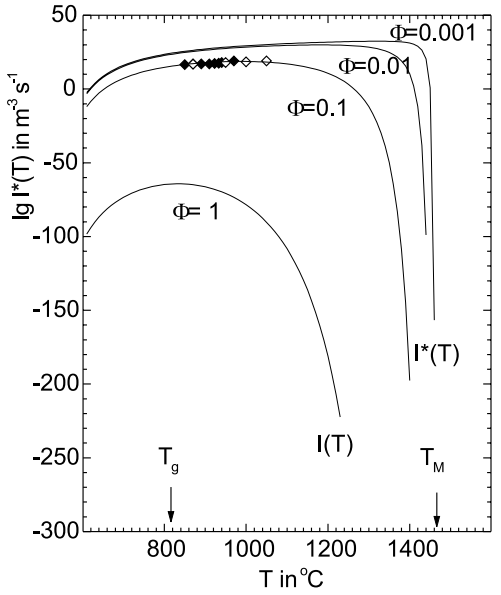

Fig. 2. Temperature dependence of heterogeneous nucleation rate. $I^*(T)$: calculated according to Eq. (1) with $W^* = W\,\Phi$ for various values of $\Phi \leqslant 1$. Experimental points were calculated from crystal size data for μ-cordierite surface crystals growing from fractured or mechanically polished cordierite glass surfaces by the Köster method [37]. Taken from [34].

nucleation rate of unpredictable temperature dependence.

Homogeneous surface nucleation. A pristine glass (or supercooled liquid) surface can be considered as ideal, if nucleation occurs with equal probability from every *surface* region. This surface nucleation rate is an inherent property of the glass–air interface. In this case, a 'homogeneous surface nucleation' rate, I^+ [1/m^2 s], can be defined. I^+ equals the experimentally obtained ('apparent') *surface* nucleation rate, $\mathrm{d}N/\mathrm{d}t$ [1/m^2 s], as expressed in Eq. (9). Surface nucleation from Pt/Rh container walls were treated in Refs. [17–19] this way. However, homogeneous surface nucleation at pristine and glass surfaces is unlikely as demonstrated by experimental evidence (see Section 3.3).

$$\frac{\mathrm{d}N}{\mathrm{d}t} \equiv I^+. \tag{9}$$

Heterogeneous surface nucleation. In most cases of practical relevance, glass surfaces are highly susceptible to the presence of nucleation sites (e.g. dust). Hence, surface nucleation could be treated as a special case of heterogeneous nucleation on some active sites. $\mathrm{d}N/\mathrm{d}t$ should be discussed in terms of Eq. (8), replacing S_V by the number of surface nucleation sites per unit area, S [1/m^2], and $\mathrm{d}N_\mathrm{V}/\mathrm{d}t$ by $\mathrm{d}N/\mathrm{d}t$ [1/m^2 s].

$$\frac{\mathrm{d}N}{\mathrm{d}t} = S I_S. \tag{10}$$

2.1.3. Surface nucleation kinetics

Using-up of nucleation sites. The kinetics of heterogeneous (surface) nucleation is complicated by the exhaustion of available nucleation sites due to crystal nucleation and growth, as illustrated in Fig. 1(b) and (c) (see Ref. [8] for a more comprehensive kinetic discussion). Eq. (11) gives the related differential kinetic equation, where S [1/m^2] is the constant number of surface nucleation sites. $\mathrm{d}N/\mathrm{d}t$ is proportional to the number density of non-used nucleation sites, $[S–N]$, and to their 'using-up' rate, I_S. Formal integration of Eq. (11) yields Eq. (12).

$$\mathrm{d}N/\mathrm{d}t = [S - N]I_S, \tag{11}$$

$$N(t) = S\left[1 - \exp\left(-\int_0^t I_S(t')\,\mathrm{d}t'\right)\right]. \tag{12}$$

Assuming a non-steady-state $I_S(t)$, according to Eq. (5), similar to I^* or I^+, Eq. (12) yields Eq. (13) [19]. $N(t)$ has sigmoid shape as illustrated in Fig. 1(c). The maximum of $\mathrm{d}N/\mathrm{d}t$, is attained at some intermediate stage of nucleation. In the most general case, the active sites can be exhausted and saturation $N = S$ can be reached before I_S attains its steady-state I_{S0} [13].

$$\begin{aligned} &N(t) = S\{1 - \exp\left[-I_{S0}t\Psi(t)\right]\},\\ &\text{with } \Psi(t) = \exp\left[-\tau/t\right] + [\tau/t]\boldsymbol{Ei}[-\tau/t]. \end{aligned} \tag{13}$$

Variable number of nucleation sites. Generally, nucleation sites that have not caused nucleation can form or disappear during nucleation treatment, as reported in Refs. [20,21]. Thus, S can depend on the annealing time and the initial S_0. To a first approximation, this process can be

described by steady-state site generation and degeneration rates, $\beta^+(T)$ and $\beta^-(T)$ [1/s], respectively. Consequently, a given kind of nucleation site can be restricted to a certain temperature range (e.g. limited by the melting point of solid contaminants). A related kinetic study is given in Refs. [23,24]. In this paper, constant (zero) β^+ and β^- are assumed. Thus, both the nucleation rate, I_S, and the deactivation rate, β^-, reduce the number of available (non-used) nucleation sites. A kinetic equation was derived based on some simplifying assumptions concerning the nucleation rate. $I_S \equiv 0$ and $I_S =$ constant were adopted for $t < \tau$ and $t > \tau$ (nucleation time lag), respectively. For $t > \tau$ it was found:

$$N(t) = S_0 \exp(-\beta^-\tau)\left[\frac{I_S}{I_S+\beta^-}\right] \times \{1 - \exp[-(I_S+\beta^-)(t-\tau)]\}. \quad (14)$$

Different kinds of nucleation sites. Finally, we assume that different kinds of nucleation sites, ***i*** (e.g. airborne dust or polishing powder particles) cause nucleation of the same crystal phase in a given glass. In this case, $S = \Sigma S_i$ and $N(t) = \Sigma N_i(t)$ hold. Due to the different activity of different kinds of sites, I_{Si} may also differ, and fitting $N(t)$ requires a full set of parameters S_i and I_{Si}. In many cases, however, surface nucleation is dominated by one type of nucleation site, which has a large number density (S_i) and/or larger nucleation activity (I_{Si}). For instance, for a given experimental condition (e.g. thermal treatments of fractured surfaces) dust particles may dominate. However, changing the experimental condition, e.g. using ground surface other kinds of nucleation sites (e.g. scratches) may govern $N(t)$. Changing the temperature range of the nucleation treatment might cause a similar change of the nucleation mechanism. It is also probable that nucleation of different crystal phases is caused by distinct kinds of active sites.

2.2. Experimental surface nucleation data

2.2.1. Experimental limits

Different experimental dN/dt data cannot be compared without full kinetic measurements up to *saturation* at $N = S$ (see Eq. (12)). The latter is often hindered by experimental limits related to the minimum size of detectable crystals, d, which in turn is determined by the experimental method (e.g. optical microscopy) and the maximum available sample surface, A. Therefore, N can be expressed more illustratively as the mean next-neighbor distance of surface crystals (or nucleation sites), $2l$, according to Eq. (15).

$$2l \approx N^{-1/2}. \quad (15)$$

The upper limit, N_U, is related to d. To ensure separate and countable crystals, d must be less than $2l.N_U \approx 10^{-1}$ μm^{-1} or $2l \approx 3$ μm are typical for optical microscopy. For two-step nucleation treatments, crystal impingement imposes an upper bound for N. For one-step nucleation treatments N_U is reached at some maximum annealing time (shadowed region on the right-hand side of Fig. 1(c)). A lower limit, N_L^A, is related to A, on which at least one crystal must occur. Thus, $N_L^A \approx 10^{-8}$ μm^{-2} or $2l \approx 10$ mm results for $A \approx 10 \times 10$ mm^2. Another lower limit, N_L^d is related to the minimum annealing time of one-step treatments allowing the growth of detectable crystals (shadowed region on the left-hand side of Fig. 1(c)). Either N_L^A or N_L^d can limit $N(t)$ measurement.

For cases of smaller nucleation activity, only few of the available nucleation sites are used-up until crystal impingement stops further measurement of $N(t)$. $N(t) < S$ holds in all stages (Fig. 1(c), curve 2). This condition is caused by either a large number of initial nucleation sites, S, or by a small nucleation rate, I_S. dN/dt can be directly measured as a function of temperature. However, S remains unknown preventing the determination of I_{S-}, which measures the nucleation activity of the dominating nucleation sites. Thus, the interpretation of dN/dt data is difficult.

Nucleation sites of greater nucleation activity are used up faster than other sites. Full saturation at $N \approx S =$ constant can even occur before any crystal reaches a detectable size (Fig. 1(c), curve 1). This state is also caused by a small number of initial nucleation sites, S, or by larger nucleation rates, I_S. In these cases, no additional (previous or future) thermal treatment may alter N, which has a defined constancy mimicking an athermal state.

2.2.2. Low nucleation activity

The few surface nucleation data known to us suffer from the above mentioned difficulties. A summary of these kinetic data is shown in Fig. 3 and the data sources for the curves are given in Table 1.

The surface nucleation of the '123'-*phase* in non-stoichiometric soda-lime-silica glasses were studied in Ref. [18]. The maximum of dN/dt (Eq. (11)), dN/dt_{max}, could be measured only in a small temperature interval where it decreased (Fig. 3, curve 2, •). However, the experiments of Ref. [18] refer to nucleation on Pt surfaces and no kinetic analyses were performed. A similar situation occurs in Ref. [17] where the surface nucleation of a soda-baria-silica glass at the Rh/Pt crucible wall was measured.

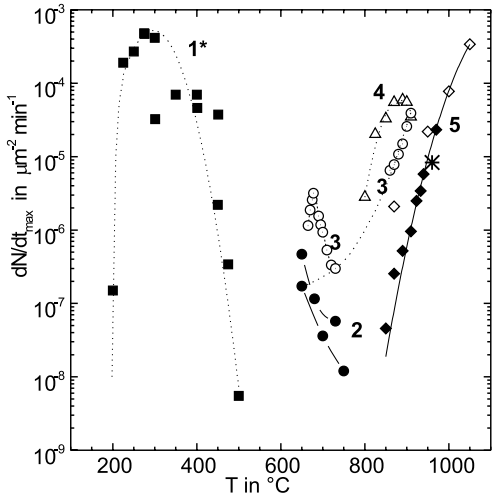

Fig. 3. Experimental surface nucleation rate data (curves 1*, 2, 3 and 4, see Table 1 for details). Curve 5 shows the surface nucleation rate of μ-cordierite in cordierite glass, obtained from crystal size data by the Köster method [37] (fractured surface: points ◇ [34], mechanically polished: points ◆ [38]). * Curve 1* is probably obscured by the additional formation and decay of nucleation sites. Taken from [34].

Full measurements of dN/dt_{max} as a function of temperature were described in Ref. [22] for the nucleation of *sodium disilicate* crystals at fire-polished surfaces of the glass of the same composition. A strong influence of the partial pressure of CO_2 in the ambient atmosphere on dN/dt was evident. However, the results indicate that the presented nucleation rate data were obscured by the kinetics of formation of surface nucleation sites. As the maximum, dN/dt_{max} occurs at 300°C that is $< T_g$ of sodium disilicate glass ($\approx$ 460°C) and X-ray measurements proved the formation of $NaCO_3$ crystals on the glass surface (from atmospheric reaction), which act as nucleation sites for the crystallization of NS_2, the nucleation data do not refer to NS_2 crystal nucleation kinetics.

A better situation was reported for *anorthite* crystals growing from the iso-chemical glass surface [25]. N increased with time tending to reach a saturation level, S, at about 0.004 μm^{-2} ($2l \approx 15$ μm). Repeated annealing have lead to a stepwise increase of S up to 0.01 μm^{-2} ($2l \approx 10$ μm). The maximum apparent surface nucleation rate, dN/dt_{max} (at 960°C, 110 K above T_g), is shown in Fig. 3 (star).

The most comprehensive surface nucleation kinetic data so far reported were obtained in Refs. [23,24,26,27] for '*X-phase*', a metastable crystal phase that grows from CeO_2-polished cordierite glass surfaces, simultaneously to the occurrence of μ-cordierite. Due to the appropriate growth rate of the X-phase crystals and the small number density of the related nucleation sites, the full $N(t)$-curve,

Table 1
Details of the measured surface nucleation data in Fig. 3. Taken from [34]

Curve	Points	Glass	Surface	Crystal	Reference
1*	■	$Na_2O \cdot 2SiO_2$	Fire polished	$Na_2Si_2O_5$	[22]
2	•	Soda-lime	Fire polished	'123'	[18]
3	⊙	Float	Fire polished	Cristobalite	[29]
4	Δ	Cordierite	Mech. polished	X-phase	[26]
	★	Anorthite	Mech. polished	Anorthite	[25]
5	◇	Cordierite	Fractured	μ-Cordierite	[34]
	◆	Cordierite	Mech. polished	μ-Cordierite	[38]

including its saturation level, could be observed. Fig. 4 shows the surface nucleation density for the X-phase (points) and μ-cordierite crystals (curve 1, ⊙) for long (310 h) nucleation anneals at various temperatures. A second anneal was applied to allow crystal growth to a detectable size (1.5 h at 930°C). I_S for X-phase crystals reaches its maximum at 890°C, ≈ 70 K $> T_g$ of the parent glass, while the surface nucleation density for μ-cordierite was not affected by these extended pre-treatments. The saturation level decreased with increasing nucleation temperature, indicating that the nucleation sites for the X-phase disappear.

Diaz-Mora et al. [28] confirmed the studies of Yuritsin [23,24] and analyzed the kinetics of both sets of data for the X-phase. They showed that the effective interfacial energy for surface nucleation is less than that for homogeneous volume nucleation in silicate glasses, vindicating the assumption of heterogeneous nucleation on free glass surfaces. The average wetting angle between the nucleating crystals and the active solid particles was estimated to be 40°. The pre-exponential constant was several orders of magnitude larger than the theoretical constants, as found for volume homogeneous nucleation in oxide glasses.

These findings illustrate that different crystal phases can be induced by different kinds of nucleation sites and that quite different nucleation rates occur in each case.

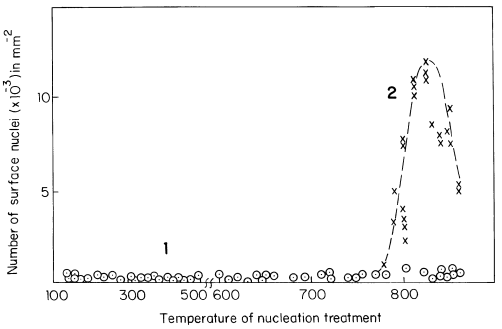

Fig. 4. Surface nucleation density at mechanically polished cordierite glass surfaces after two-stage nucleation and growth treatments 1: μ-cordierite, 2: X-phase. Nucleation treatment 310 h at different temperatures (abscissa), crystal growth treatment 1.5 h at 930°C. Taken from [26].

The nucleation kinetics of *cristobalite* at the atmosphere side of a float glass was studied in Ref. [29]. At low temperatures ($\leqslant 700$°C), long induction times (> 2 h) were observed and N increased to 2000 mm^{-2} ($2l \approx 20$ μm). dN/dt_{max} was maximized at 670°C (≈ 100 K above T_g) and decreases at higher temperatures (Fig. 3, curve 3, group of points ⊙ at the left). At temperatures $T \geqslant 850$°C, however, the nucleation activity increased again. Induction periods were undetectably short and N reached saturation at 500 mm^{-2} ($2l \approx 45$ μm) within 60 min (Fig. 3, curve 3, upper group of points ⊙). This effect illustrates that different kinds of nucleation sites can cause nucleation of the same crystal phase with different nucleation rates and saturations.

2.2.3. High nucleation activity

Saturation. Examples of saturation of $N(t)$ were found on free glass surfaces. An observation of unchanged N with respect to the nucleation treatment, was found for the surface crystallization of *Zr–Ba–La fluoride glass* [30]. Unfortunately, no quantitative data of N were given. A first measurement of constant N was given for an almost stoichiometric *diopside* glass [31,32]. In the case of CeO_2 polished surfaces, $N \approx 8 \times 10^{-2}$ μm^{-2} ($2l \approx 4$ μm) for all nucleation treatments tested.

A similar observation was made for μ-*cordierite* on polished [26] (Fig. 4, curve 1, ⊙) and fractured cordierite glass surfaces [33,34] (Fig. 5) for two-step and one-step nucleation treatments, respectively. $N \approx S \approx 10^{-4}$ μm^{-2} ($2l \approx 10$ μm) was found in both cases. Neither rapid heating (at 1000 K/min) to temperatures of crystallization [34] nor prolonged nucleation treatments [26] altered N.

Analogous situation was observed for the nucleation of *devitrite* and *diopside* on float and microscopic slide glass surfaces [35,36]. N scattered between '0 = not observable' and 3000 mm^{-2} ($2l =$ '∞' -18 μm), particular to each type of surface preparation, without any effect of the nucleation annealing time. For *devitrite* crystals on as-received microscope slide glass surfaces, N varied from 800 to 3000 mm^{-2} ($2l \approx 35$–18 μm). A variable number of nucleation sites, such as dust or polishing powder particles, might explain the data

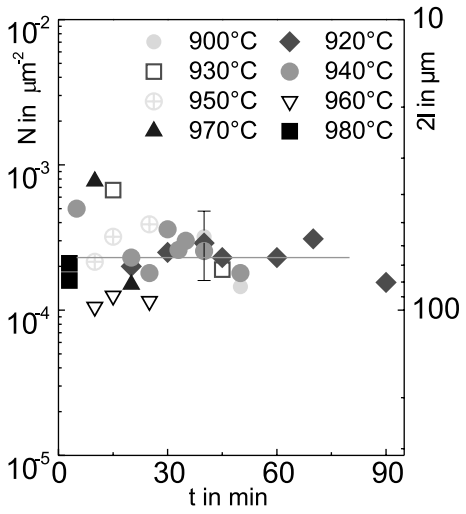

Fig. 5. Nucleation density of μ-cordierite crystals at fractured cordierite glass surfaces, N, for one-step thermal treatments at different temperatures (symbols) in the free atmosphere as a function of annealing time, t. The related next neighbor distance, $2\ell = N^{-1/2}$, is given for illustration. Taken from [33].

scatter in all these cases, confirming that N varies with S.

Indirect measure of dN/dt (*Köster's method*). For saturation, dN/dt cannot be directly measured. Large crystals grow to almost uniform size as illustrated in Fig. 6(a). Nevertheless, the kinetics of using-up nucleation sites can cause a distribution of crystal sizes for the same system (Fig. 6(b)). The fact that the first nucleated crystals grow to larger size than the latest born crystals, clearly indicates that nucleation is not '*athermal*', but spread over a period of time.

This effect allows an indirect estimation of dN/dt [37]. If t_i denotes the nucleation time of a crystal i and dr/dt the linear crystal growth rate, the diameter deviation between two crystals, $\Delta \mathrm{d}_{ij}$, is simply due to the interval, Δt_{ij}, between the related nucleation events, according to Eq. (16). The number of crystals within the diameter range $\Delta \mathrm{d}_{ij}$ is a consequence of dN/dt within Δt_{ij}. The maximum diameter deviation, Δd_{M}, gives the time interval between the 'first-and last-born' crystal and thus of the time required to exhaust all nucleation sites, Δt_{M}.

$$\Delta \mathrm{d}_{ij} = \Delta t_{ij} 2\mathrm{d}r/\mathrm{d}t. \tag{16}$$

The crystal size distribution is best detected at $t \approx t_{\mathrm{M}}$ when all nucleation sites are just used-up. For $t < \Delta t_{\mathrm{M}}, \Delta d_{\mathrm{M}}$ and the number of crystals are both increasing. This situation is indicated in Fig. 7 by increasing cumulative bar graph areas and half-widths for increasing annealing times. Further crystal growth at $t > \Delta t_{\mathrm{M}}$ does not change Δd_{M} but increases the average crystal size $\langle d \rangle$, as illustrated in Fig. 8. In this case the crystal size distribution can be obscured by a larger mean crystal size ($\langle d \rangle \gg \Delta d_{\mathrm{M}}$) and by crystal morphology phenomena.

Köster's method was applied to the nucleation of μ-cordierite at fractured [34] and polished [38,39] cordierite glass surfaces. d$N(T)$/d$t_{\max}$ is shown in Fig. 3 (curve 5, points ◆ [38] and ◇ [34]) together with directly measured dN/dt data (of unknown saturation level). Despite the saturation effect for μ-cordierite ($S_\mu \approx 10^{-4}$ μm^{-2} was found in both cases) dN/d$t_{\max}$ (curve 5) is within the scatter limits of the combined data (curves 2–4). Thus, saturation was not solely caused by large dN/dt, as we intuitively expected (see Section 2.3 for further discussion).

2.3. Temperature range of nucleation

Volume nucleation. For systems that have *homogeneous* volume nucleation, the experimental temperatures of the maximum nucleation rate, $T_{\max}$, are always at or $> T_{\mathrm{g}}$, and $T_{\mathrm{g}}/T_{\mathrm{f}}$ is 0.54–0.50 [9] (T_f is the melting point of the crystal). One of us [40] showed that, for homogeneous nucleation, the calculated (by CNT) $T_{\max}$ is also close to T_{g}. It was later demonstrated for 12 oxide glasses that the reverse also applies, e.g. if the predicted $T_{\max}$ (for homogeneous nucleation) is $< T_{\mathrm{g}}$, only surface or heterogeneous nucleation is observed in laboratory time scales [41]. For several glasses, which fall into the latter category, the failure to undergo homogeneous nucleation must be attributed to their low nucleation rate or to long transient nucleation times.

Heterogeneous volume nucleation is employed to achieve fine grained glass-ceramics, and certain nucleating aids, such as TiO_2, ZrO_2 and P_2O_5 (e.g. [42]) have been studied. These oxides, however, cannot be simply considered to provide nucleation

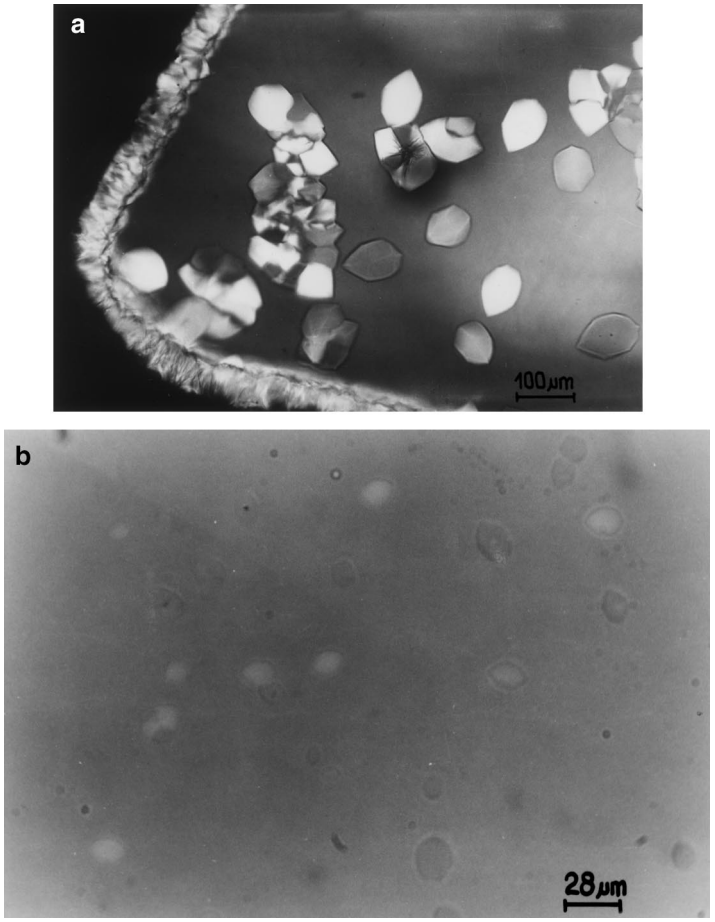

Fig. 6. μ-Cordierite crystals nucleated at fractured glass surfaces. Transmission optical micrographs, top view under slightly crossed nicols: (a) large crystals almost uniform in size, after annealing for 30 min at 960C, (b) small crystals of various size after annealing for 10 min at 950°C. Taken from [34].

sites because they are used in relatively large quantities (2–15%). Then, the properties of the parent glass also change and nucleation data for both the basic and modified glasses are not comparable. A similar difficulty appears for glasses melted in steam atmosphere to cause gas bubbles that trigger nucleation [43,44].

Because of the detailed nucleation studies for the base glass, only heterogeneous bulk nucleation of cordierite glasses ($2MgO \cdot 2Al_2O_3 \cdot 5SiO_2$) containing TiO_2 is mentioned here. Glasses having more than 4–8 wt% have volume nucleation [3,39] due to the precipitation of a titanium rich crystalline phase [45]. The temperature of maximum nucleation rate for μ-cordierite (Fig. 9, curve 1, points ○) and indialite (Fig. 9, curve 2, ●) occur 50 K below and in the vicinity of the glass transition temperature ($T_g \approx 770$°C), respectively. Unfortunately, the theoretical T_{max} was not estimated for these phases.

Surface nucleation. Strong nucleation activity is evident between 70 and 110 K above T_g from directly measured surface nucleation rate data (Fig. 3). This finding confirms well the temperature dependence of I^* predicted by CNT, as shown in Fig. 2, and indicates a strong nucleating efficiency of surface nucleation sites. The same efficiency is observed for indirectly obtained dN/dt data for

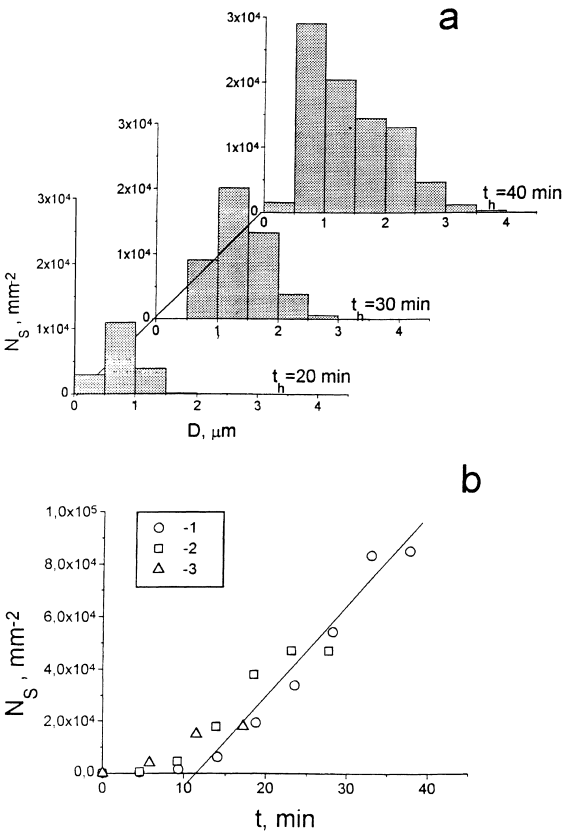

Fig. 7. (a) Size distributions of μ-cordierite crystals nucleated at diamond-polished surfaces of cordierite glass (containing 8.14 wt% TiO_2) after annealing at 850°C for $t_h = 20$, 30 and 40 min. (b) Calculated time dependence of $N(t)$ for these treatments ($t_h = 20$ min: △, $t_h = 30$ min: □,$t_h = 40$ min: ○). Taken from [39].

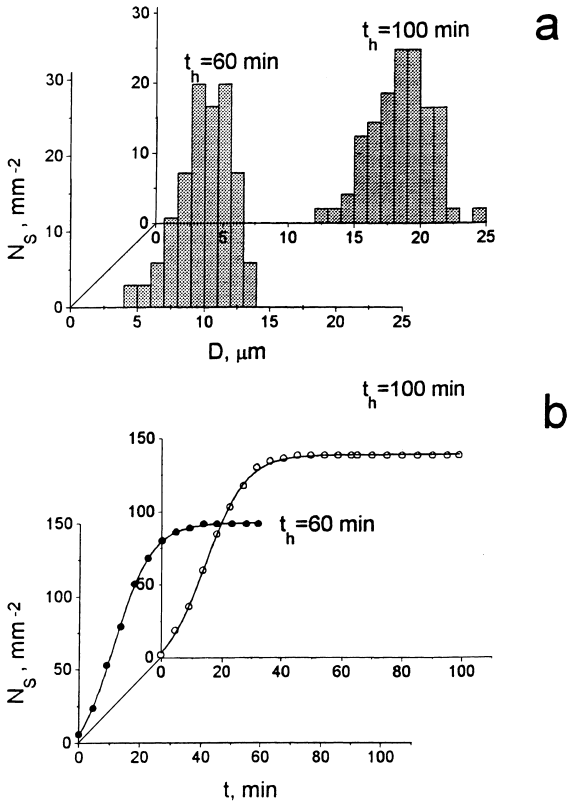

Fig. 8. (a) Size distributions of μ-cordierite crystals nucleated at diamond-polished surfaces of cordierite glass (containing 1.21 wt% TiO_2) after annealing at 850°C for $t_h = 60$ and 100 min. (b) Calculated time dependence of $N(t)$ for these treatments ($t_h = 60$ min: ●, $t_h = 100$ min: ○). Taken from [39].

μ-cordierite. dN/dt increases to 1050°C, which is 235 K $> T_g \sim 815$°C. The latter finding corroborates the strong nucleation efficiency of the surface nucleation sites, as well as for a broad temperature range for their existence (probably refractory dust particles, e.g. Al_2O_3). A similar property was found in [29] for the nucleation of Cristobalite at float glass surfaces.

This broadening of the nucleation curve could be fitted in terms of the CNT. This fitting is illustrated in Fig. 2, where dN/dt data were taken from Fig. 3 to calculate I^* (see Ref. [15] for detail). As shown in Fig. 10, the crystal growth rate, dr/dt, is larger in this temperature range and has a similar temperature dependence as dN/dt. In this case, any thermal treatment allowing the growth of detectable crystals will deplete nucleation sites. This depletion is the main obstacle for both successful study and technological control of N via two-step nucleation and growth treatments and, therefore, is responsible for the observed constancy of N for μ-cordierite.

Simultaneous interior and surface nucleation. Direct experimental data for both volume and surface nucleation in the same glass are rare to our knowledge. Previous data were reported in Ref. [18] for a non-stoichiometric soda-lime-silica glass and in Ref. [17] for soda-baria-silica glass, where surface nucleation was observed at higher temperatures than those for interior nucleation. However, dN/dt decreased with increasing

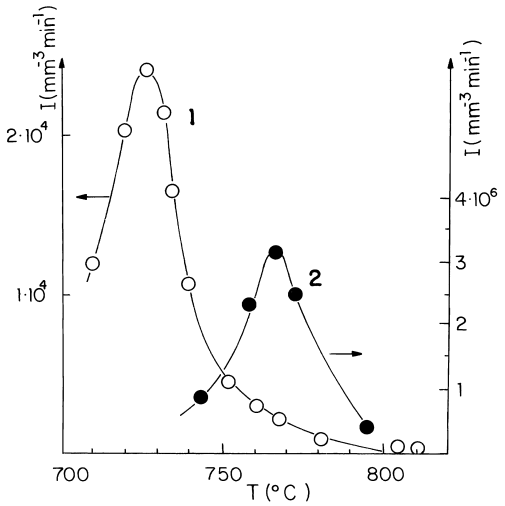

Fig. 9. Heterogeneous volume nucleation rate of μ-cordierite (1) and indialite (2) in a cordierite glass containing 10 wt% TiO_2. Taken from [95].

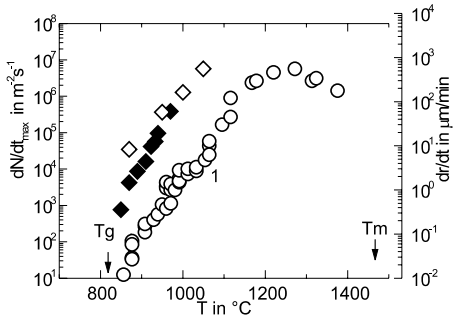

Fig. 10. Temperature dependence of the maximum surface nucleation and crystal growth rates for μ-cordierite in cordierite glass. Surface nucleation rate, dN/dt_{max}: obtained via Kösters' method [38], ◇: fractured surface of cordierite glass [34], ◆: mechanically polished surface of cordierite glass [38]). Crystal growth rate, dr/dt: ○ [34]. Arrows: T_g = transition temperature at 815°C [34]; T_M = melting point of the high temperature polymorph of cordierite at 1467°C [94]. Figure taken from [93].

temperature and the temperature of maximum nucleation was not given. Additionally, no kinetic analyses were performed in Refs. [17,18].

More recently, systematic measurements and kinetic analyses of surface nucleation and growth of μ-cordierite on diamond polished surfaces and on fractured surfaces of cordierite glasses containing 0.3, 1.2, 3.4, 6.2 and 8.1 wt% TiO_2 were carried out [39]. All glasses have surface nucleation; however, the glass having 8.1 wt% TiO_2 also has volume nucleation. It was shown that both surface and volume crystallization occur by heterogeneous nucleation. Fig. 11 compares the measured (apparent) volume and surface nucleation rates. We expect the maximum temperature of the (heterogeneous) surface nucleation rate (● in Fig. 11) to be at $T > 880$°C, which is considerably above the temperature of the maximum heterogeneous volume nucleation rate (○ in Fig. 11). The substrate activities, Φ, were estimated from surface and volume nucleation measurements. The widely different Φs indicate that the active catalyzing sites are not the same for surface and volume crystallization. The authors [39] reasonably assumed that volume crystallization of μ-cordierite is induced by Al_2TiO_5 crystals, while surface crystallization is affected by TiO_2 as well as by defects and relicts of polishing powder.

In summary, the above described findings and the fact that, in most cases, surface nucleation occurs at temperatures far above T_g indicate that surface nucleation sites are more efficient ($\Phi \ll 1$) than interior nucleation sites. This difference is confirmed by the well-known experience that, even when volume nucleation is promoted by nucleating agents or pre-treatments, a crystal surface layer is present.

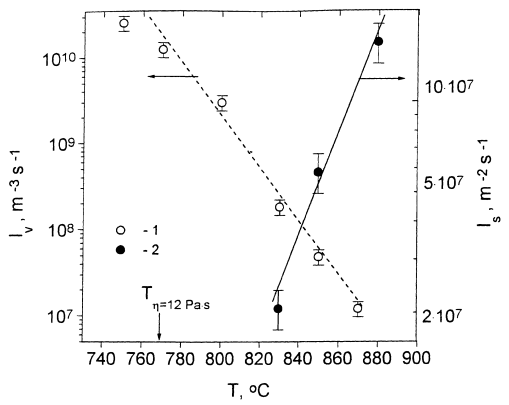

Fig. 11. Stationary heterogeneous volume nucleation rate, I_V (○; in the sense of $dN_V/dt \approx S_V I_S$ in Eq. (8)) and the apparent surface nucleation rate, I_S (●; in the sense of $dN/dt \approx SI_S$ in Eq. (10)). Straight lines are placed to guide the eye. Taken from [39].

3. The surface nucleation sites

Because surface nucleation kinetics are governed by the presence of nucleation sites, the knowledge and understanding of their properties is a key issue in controlling surface crystallization. Unfortunately, the *nucleation mechanisms* are still a matter of controversy (see e.g., Refs. [46–60]). Nucleation can be catalyzed by decreasing the thermodynamic barrier (e.g., decreasing σ with surfactants or substrates[46]) or the kinetic barrier (decreasing η due to volatilization or contamination). Elastic stresses [47] or local shear strain [48] may also have effects. Accordingly, the several types of surface nucleation sites are discussed in terms of a variety of physical and chemical phenomena.

For instance, Tabata [49] argued that surface regions of smallest radius of curvature are preferred nucleation sites due to the increased molecular mobility in these regions. Selective volatilization from the external surfaces were proposed in Ref. [50] to cause surface nucleation. Swift [51] proved that airborne dust triggers surface nucleation. Mattox [52] discussed that effect for graphite particles coming from the mold. In Refs. [24,53] the hydrolytic attack of water was discussed to promote surface nucleation. Elastic stress phenomena were claimed to hinder bulk crystallization to a greater extent than surface crystallization and hence to promote the latter [47]. In terms of that concept, strong nucleation activity was predicted for sharp convex edges and small glass particles. (Elastic strain phenomena were also addressed to prevent heterogeneous bulk nucleation at very small metal particles ($\lessapprox$10 nm) [54]). In [55] and [48], increased nucleation rates were attributed to shear strain phenomena.

Various *difficulties* complicate the study of the nucleation mechanism. Experimental limitations prevent micro-analytical evidence of the former nucleation sites (e.g. healing of cracks, dissolution of dust particles). The experimental limits of the determination of $N(t)$ (see Section 2.2.1) often prevent the measurement of S. This quantity must be known for comparison of nucleation data of different systems and for the understanding of external parameters, such as surface condition or annealing atmosphere. Several kinds of nucleation sites, differing in number density and activity, may occur simultaneously. Additionally, the glass surface cannot be described using interior properties in any case (e.g. due to unsaturated chemical bonds, evaporation, corrosion). Finally, the statistical properties of surface nucleation sites (e.g. scratches, dust) causes data scatter, which can obscure the effect of many parameters, and requires control of reproducible surface preparation and ambient annealing conditions. Moreover, it should be stressed that many nucleating mechanisms can act simultaneously in various proportions as a function of glass composition, surface preparation, temperature range of nucleation, annealing condition and other parameters.

We consider: (i) *mechanical damage* (due to the potentially large number density of surface defects), (ii) *dust* particles (due to their non-avoidable, random occurrence), and (iii) the *annealing atmosphere*. As in the last section, glasses having pronounced crystallization tendencies are preferentially studied because they are interesting for the development of glass-ceramics. Undesirable devitrification of stable glasses proceeds slowly. In this case, the melt surface has higher reactivity (e.g. compositional changes, dissolution of dust) and other nucleating mechanism may dominate.

3.1. Mechanical damage

3.1.1. Surface roughness

Mechanical damage is known to promote surface nucleation of glass. In [56], surface damaging was applied to increase the mechanical strength of vitreous materials by the crystallization of fine-grained surface layers. Partridge [57] and McMillan [1] reviewed surface crystallization of glasses with different types of surfaces. Ding et al. [58] achieved fine-grained, transparent crystalline surface layers for optical application by means of surface damaging via ultrasonic treatment with an aqueous suspension of small grains of the desired crystal phase previously to thermal treatment. (This effect could not be achieved in [59] for SiO_2–Na_2O glass by rubbing or grinding with devitrification products.)

Table 2 summarizes surface nucleation density (N) for damaged glass surfaces showing a strong dependence of N upon the degree of surface roughness. Smaller N, down to $\approx 5 \times 10^{-8}$ μm^{-2} ($2l$ up to ≈ 5 mm) frequently occur at freshly fractured surfaces. This N is illustrated in Fig. 12 for a cordierite glass surface fractured and thermally treated in vacuum. Low N is also typical for fire-polished glass surfaces. Medium N, between 10^{-3} μm^{-2} ($2l \approx 30$ μm) and 10^{-6} μm^{-2} ($2l \approx 1$ mm) are evident on mechanically *polished* or *fractured* surfaces in standard laboratory atmosphere. The data scatter is probably due to the presence of dust particles (see Section 3.2). Larger N, up to 10^{-1} μm^{-2} ($2l \approx 3$ μm), are reported for ground or glass powder surfaces, as illustrated in Fig. 13.

3.1.2. Corners, edges and tips

The nucleation mechanism related to mechanical damage is not well understood to date. As mentioned above, Tabata [49] observed for several silicate glasses that surface nucleation is promoted by '*sharp edges or cicatrices*'. He argued that surface tension is the governing factor of surface nucleation and that the nucleation rate is increased by improved molecular mobility in the vicinity of surface with the smallest radii. Ernsberger [60] showed for plate-glass that crystals are preferably located at the cross-points (and therefore at the edges) of macro cracks (see Fig. 9 in [60]).

More recently, as schematically illustrated in Fig. 14(a) we confirmed for cordierite, diopside, lithia-alumina-silica and float glasses that *sharp edges or tips* are favored nucleation sites [61–65]. Thus, surface crystals preferably occur along surface edges caused by fracturing [61], along the edges of cracks caused by rapid cooling of glass ribbons [62,63] or along diamond-made surface scratches [64–66]. Sometimes, double chains of crystals nicely form along the faced scratch edges, as illustrated in Fig. 15(a) and (b). Glass particles dusted on a fractured glass surface, or those caused by sample fracturing were found to trigger crystallization at the contacted glass surface [39,62,63,67]. Thus, under clean conditions, particles having the composition of the parent glass

Table 2
Surface nucleation densities, N, of damaged glass surfaces[a]

Surface	Glass	Crystal	N (μm^{-2})	2ℓ (μm)	Reference
Powder	$M_2A_2S_5$	μ-Cordierite	10^{-3}–10^{-1}	30–3	[4]
Ground	$M_2A_2S_5$	μ-Cordierite	0.2×10^{-2}–7×10^{-2}	22–4	[33]
	CZA_2S	Willemite	3×10^{-2}	6	[1]
Mech. polished	$M_2A_2S_5$	μ-Cordierite	1×10^{4}–10×10^{-4}	100–30	[33]
			2×10^{-4}	70	[23]
	CZA_2S	Willemite	1×10^{-3}–3×10^{-3}	30–18	[1]
	Diopside	Diopside	6×10^{-2}–10×10^{-2}	1–3	[32]
	Anorthite	Anorthite	1×10^{-3}–4×10^{-3}	30–7	[25]
	NC_3S_6	Devitrite	1×10^{-1}	3	[36]
	Non-stoich.	β-Wollastonite	5×10^{-5}–10×10^{-5}	140–100	[36]
	Devitrite	Tridymite	5×10^{-5}–10×10^{-5}	140–100	[36]
	Devitrite	Devitrite	1.5×10^{-4}–7×10^{-4}	80–38	[36]
	Mic. slide	Devitrite	1×10^{-4}–6×10^{-4}	100–40	[36]
As-received	Float	Devitrite	3×10^{-4}–30×10^{-4}	58–18	[36]
	Float	Diopside	5×10^{-5}	140	[36]
	Float	Tridymite	1×10^{-5}	316	[36]
	Mic. slide	Devitrite	8×10^{-4}–30×10^{-4}	35–18	[36]
Fractured	$M_2A_2S_5$	μ-Cordierite	10^{-3}–10^{-8}	30–5000	[64]
			10^{-5}–10^{-6}	300–1000	[23]
Fire-polished	Mic. slide	Devitrite	'0'	'∞'	[36]
	$M_2A_2S_5$	μ-Cordierite	'lowest'		[92]

[a] The next neighbor distances, $2\ell \approx N^{-1/2}$ (rounded values) are presented for the sake of illustration. Taken from [93].

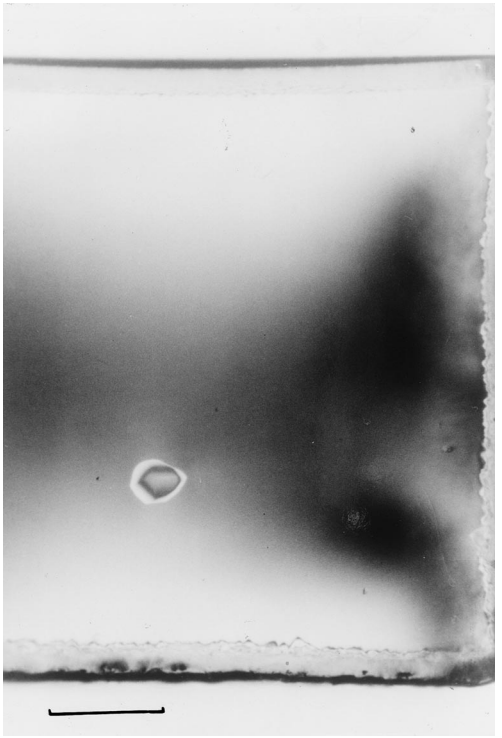

Fig. 12. Low surface nucleation density ($N \approx 6 \times 10^{-8}$ μm^{-2}, $2\ell \approx 4$ mm) at a cordierite glass surface fractured and annealed (980°C, 30 min) in vacuum. Top view optical micrograph, crossed nicols. Bar = 500 μm. A compact crystalline surface layer additionally grew from the SiC-ground surfaces of the sample. Taken from [93].

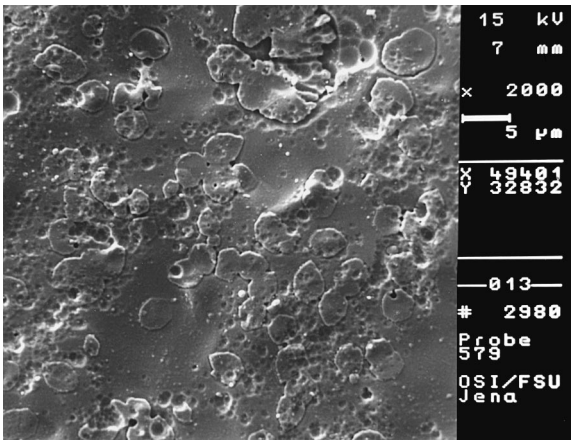

Fig. 13. High surface nucleation density ($N \approx 4 \times 10^{-2}$ μm^{-2}, $2\ell \approx 5$ μm) at a ground cordierite glass surface annealed (950°C, 7 min) in free air. Top view electron micrograph of the annealed and then slightly HF-etched surface. Taken from [93].

were detected on the center of most of the very few crystals nucleated at the fractured surface of cordierite glass. For a given glass powder sample (all particles were exposed to identical milling conditions), the surface nucleation density, N, increases with decreasing particle size because small glass particles provide a larger number of sharp edges per surface area [4].

For μ-cordierite crystals nucleating on mechanically damaged cordierite glass surfaces, other experiments show that N is correlated to the number density of surface edges or tips, whereas the condition of damaging has minor influence. This finding indicates an intrinsic (e.g. physical) nucleating mechanism, which is not restricted to particular conditions of tip generation (e.g. chemical reaction or mechanical activation). Thus, even surface edges produced by HF etching of ground glass surfaces, were found to be preferred nucleation sites [61]. At SiC-ground glass surfaces N is not affected by the applied load and grinding media (water, organic liquids). Instead, N merely increases with the number density of surface scratches caused by decreasing SiC-particle size [33]. On the other hand, a controlled reduction of N can be obtained by surface smoothening. Thus, HF-etching of ground surfaces prior to the thermal treatment strongly decreases both the number of these edges and N. $2l(\approx N^{-1/2})$ and the mean linear distance between surface tips (detected by mechanical surface-profiling) are reduced quite similarly [61]. Accordingly, polishing of SiC-ground glass surfaces reduces N with polishing time, approaching invariance at $t > 5$ min [65]. Optical and electron micrographs show that for $t > 5$ min all tips and edges of the ground surface are eliminated.

3.1.3. Elastic stress and surface nucleation

Hypothesis. A simple nucleating mechanism of convex edges or tips was suggested in [47] based on the visco-elastic nature of glass-forming melts. It was shown that elastic stress, caused by the growing crystalline clusters can substantially hinder nucleation if the density of the crystal deviates

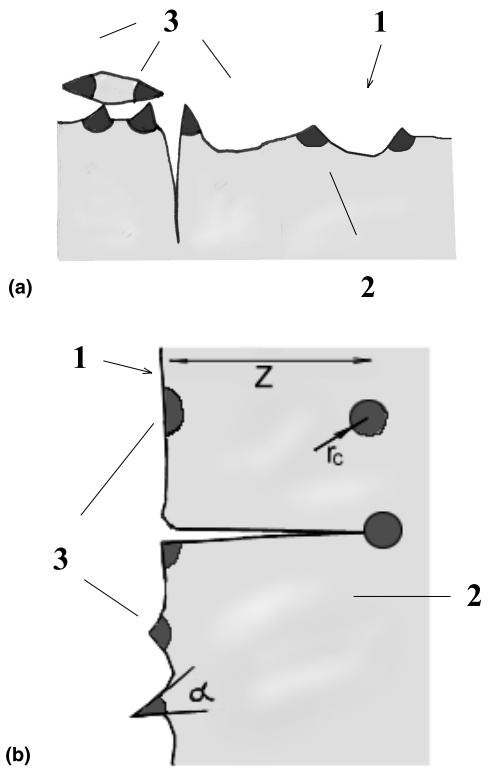

Fig. 14. (a) Schematic representation of surface tips or edges as privileged nucleation sits and (b) illustration of the effect of elastic strain on nucleation. 1: glass surface, 2: glass bulk, 3: surface crystals, Z: distance to the surface, r_c: critical radius, α: surface tip angle.

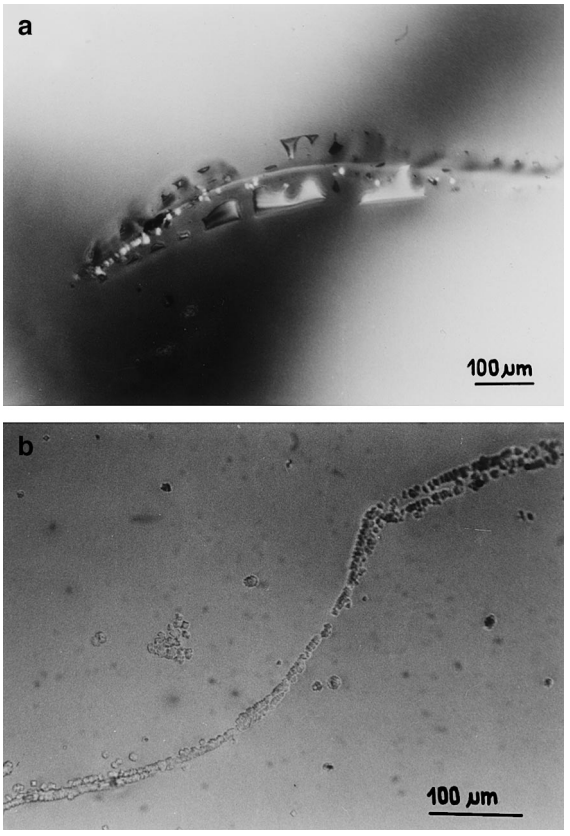

Fig. 15. Large cracks caused by rapid cooling of cordierite glass ribbons (left side: cross-section, as-received ribbon) do not cause nucleation after annealing (1000°C, 10 min, right side). Incident light micrographs, Bar = 250 µm [91].

from the melt density. Calculations are based on Eq. (17), which describes the elastic energy Φ_0, required for addition of one monomer of volume, v_C, in the glass interior,

$$\Phi_0 = \left(\frac{E}{9(1-\gamma)}\right)\delta^2 v_C. \tag{17}$$

The term $E/9(1-\gamma)$ represents the effect of the elastic properties (E = Young's modulus, γ = Poisson's number) and $\delta = (\rho_C - \rho_G)/\rho_G$ is the relative density deviation between the melt and the crystal. Neglecting stress relaxation, all elastic energy is accumulated to the cluster size α according to $\Phi(\alpha) = \alpha\Phi_0$. Hence, the molar free enthalpy change of crystallization is $\Delta\mu^{(\varepsilon)} = \Delta\mu - N_A\Phi_0$ and the corrected volume nucleation rate, $I^{(\varepsilon)}$, is given by Eq. (18) [47].

$$I^{(\varepsilon)} = I\exp\left\{-\frac{[(\Delta\mu/\Delta\mu^{(\varepsilon)})^2 - 1]W}{kT}\right\}. \tag{18}$$

As Φ_0 decreases with decreasing ratio between the distance from the surface and the cluster radius, nucleation is easier near the surface than in the interior due to the less intensive stress field in its vicinity [63]. This effect of elastic stresses is larger for sharp *convex* surface curvature such as surface edges or tips, as illustrated in Fig. 14(b).

Experimental evidence. This hypothesis explains well all results mentioned in Section 3.1.2.

Other observations support this hypothesis more directly:

(i) Large cracks (see e.g., Fig. 16), caused by quenching of cordierite glass ribbons, were completely healed during a thermal treatment [62,63,67]. The former tips did not cause nucleation. This effect confirms the model proposed in [47] because the elastic response of the glass matrix at the crack tips is nearly the same as for any other point in the interior. Tabata's [49] idea of improved molecular mobility at points of smallest curvature radii cannot explain the latter finding.

(ii) In contrast to the sharp edges of fractured glass surfaces, smooth or wavy surface curvature causes less intensive surface nucleation [61]. Correspondingly, it was shown in Ref. [63] that the energy of elastic deformation depends on the angle of convex surface tips or edges. Thus, despite the increasing number of edges per surface area for fine powders, the increased N reported in Ref. [58], can also be attributed to the well-known change of particle shape with decreasing grain size, providing a larger number of sharp edges.

(iii) The observed nucleation activity along former edges of cracks [63], scratches or Vickers' indentations [65,66] is larger for the largest δs. Fig. 17 shows the nucleation on two glass surfaces after Vickers indentation. Less numerous cristobalite crystals grow at the edges of the indentation on the float glass surface ($\delta \approx 10$)% than diopside crystals growing at the indentation edges on the diopside glass surface ($\delta \approx 15$%). In the case of μ-cordierite growing on the cordierite glass surface ($\delta \approx 2$%), indenting did not cause additional surface nucleation. Different nucleation activity of diamond-made surface indentations is presented in Fig. 17(a) and (b) for μ-cordierite and diopside, respectively.

Quantitative estimations. The role of elastic stresses on crystal nucleation in supercooled liquids can be discussed in terms of Eqs. (1)–(4), (17) and (18) [68]. A strong influence is predicted for glasses having high elastic response, $E > 90$ GPa. Thus, for diopside crystals nucleating in diopside glass ($\delta = 15$%, $E \approx 99$ GPa [68]) $I_{\max}/I_{\max}^{(\varepsilon)} \approx 10^{20}$ [65]. Even for μ-cordierite crystals growing in cordierite glass ($\delta = 2$%, $E_8 \approx 97$ GPa), $I_{\max}/I_{\max}^{(\varepsilon)} \approx 10^5$ results. On the other hand, a smaller effect of elastic stress is predicted for glasses having $E < 70$ GPa. Thus, for '123' crystals growing in soda-lime-silica glass ($\delta \approx 2$%, $E \approx 67$ GPa [65,69]) $I_{\max} \approx I_{\max}^{(\varepsilon)}$ and, accordingly, volume crystallization is easily detected in this glass.

Finally, however, we note that these estimates neglect the effects of stress relaxation. We could

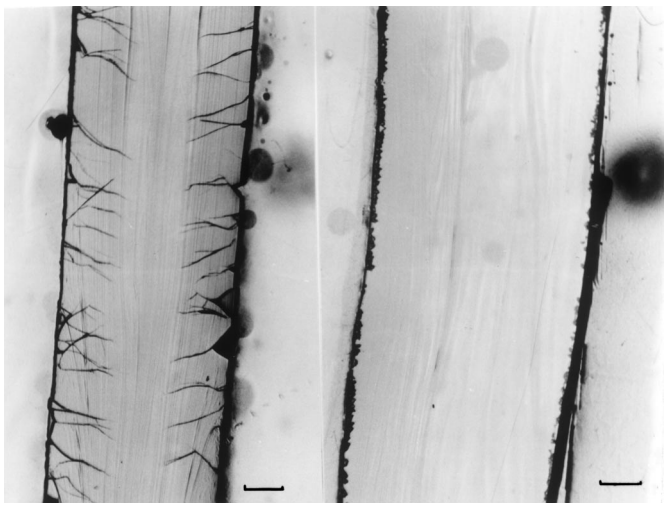

Fig. 16. μ-Cordierite ((a), 950°C, 20 min) and diopside crystals ((b), 830°C, 210 min) grown preferably along sharp edges of diamond made scratches on fractured surfaces of the iso-stoichiometric glass (optical micrographs). Taken from [65].

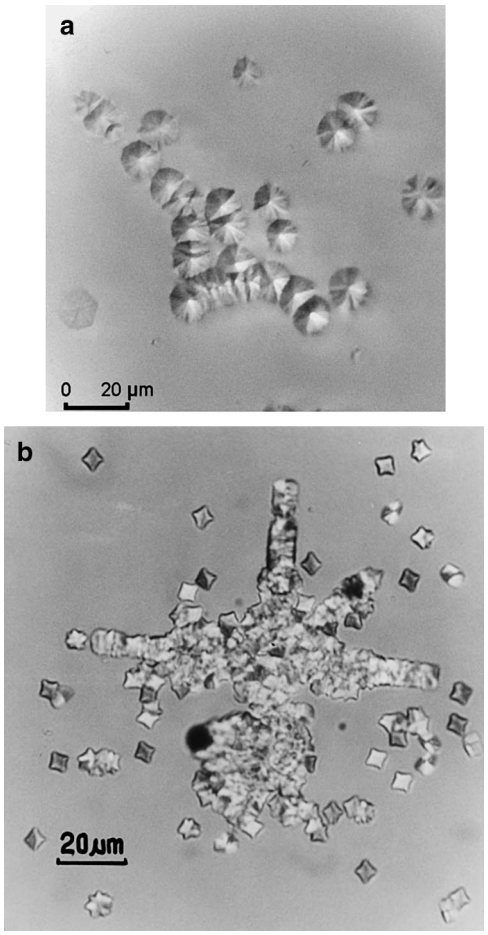

Fig. 17. Nucleation activity along Vickers indentations. (a) Cristobalite crystals growing at float glass surface annealed at 750°C for 180 min. (b) Diopside crystals growing from a polished diopside glass surface annealed at 850°C for 45 min. Optical micrographs. Relative density deviations: $\delta_{\text{diop.}} = 14.9\%$, $\delta_{\text{crist.}} = 10.4\%$. Taken from [65].

speculate that the formation of each nucleus involves small molecular units and occurs before stress relaxation. The usual comparison of average (stress) relaxation times, $\tau_{\text{rel}} = \eta/G$, with the nucleation transient times, t_{ind}, which gives $\tau_{\text{rel}} < t_{\text{ind}}$ for all temperatures, may be mistaken because nuclei are born well before a regime of steady-state nucleation is achieved. The above discussed phenomenon is controversial and deserves further experimental and theoretical efforts.

3.2. Solid particles

For smooth glass surfaces (as received, polished or fractured), N is strongly affected by the *presence of solid particles*. Thus, as early as 1739, Réaumur [70] triggered surface nucleation of glassware by contamination with foreign solid particles. Swift [51] studied crystallization of devitrite in soda-lime glass from fractured surfaces in filtered air. He suggested that air-born dust particles are a major contributing factor promoting surface devitrification. Particles of pre-crystallized glass particles were utilized to increase crystallization of powdered [71] or solid glasses [58]. Neely [72] concluded from the low nucleation activity of internal gas bubbles in soda-lime glass that the external surfaces more readily crystallize due to contamination (or volatilization). Zanotto [36] summarized related papers and showed that devitrification on bubbles only starts from solid precipitates at their wall (see also [73–75]).

More recently, solid particles were frequently found at the center of μ-cordierite surface crystals growing from slightly damaged cordierite glass surfaces (Fig. 18) [64]. Fig. 19 shows that there is a strong scatter of N due to the random occurrence of dust for different furnace materials, dust protection, or vacuum. A scatter of 7 orders of magnitude in N occurs in fire-clay furnaces, while this scatter was slightly less using gas-dense quality corundum furnace and much smaller when silica glass was used as the furnace material. A strong scatter of N was also observed for surface crystallization of diopside and devitrite [31,36].

Nucleation activity. The impact of solid foreign particles does not merely depend on their number, but is also determined by their nucleating activity. For example, microscopic observations show that numerous solid particles resting on glass surfaces during the crystallization treatment did not cause nucleation. The nucleating efficiency of solid metal substrates, Φ, have been studied for heterogeneous volume nucleation [7,76,77]. A comprehensive model is given in Ref. [46] connecting Φ with the cohesion forces in the substrate and lattice misfit. The observed decrease of Φ for increasing deviation between the thermal expansion of the

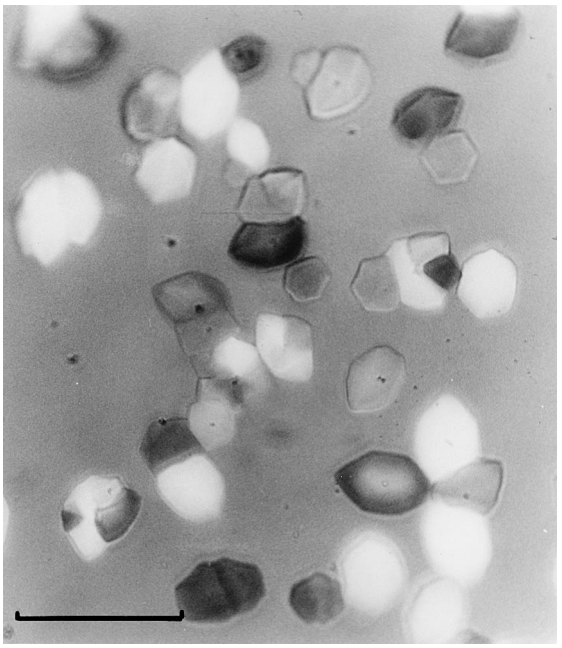

Fig. 18. Top view optical micrograph of a cordierite glass surface fractured and subsequently annealed in a conventional laboratory furnace at 960°C for 15 min. Solid foreign particles are shown in the center of surface crystals. Others have not initiated surface nucleation. Slightly crossed nicols.

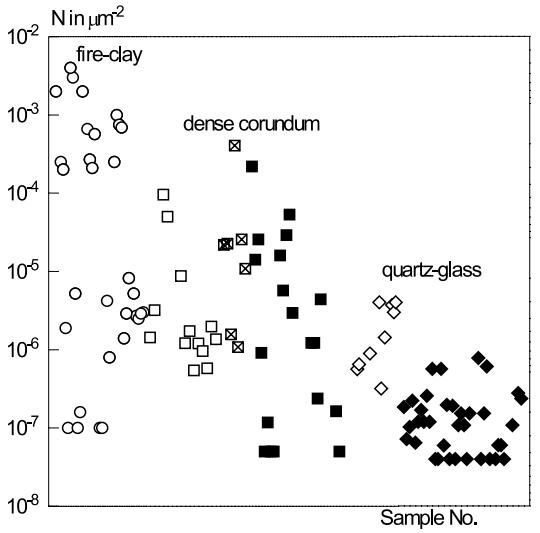

Fig. 19. Nucleation density of μ-cordierite, N, at cordierite glass surfaces, fractured and annealed under differently clean conditions. Points: ○ = fire-clay furnace, air; □ = Corundum tube furnace, air; ⊠ = Corundum tube furnace, dust protected, ■ = Corundum tube furnace, dry air; ◆ = Quartz-glass tube furnace, air: ◇ = Quartz-glass tube furnace, vacuum. Taken from [93].

substrate and the crystal [76], and for increasing melting temperature of the substrate material (see e.g. Table 1 in Ref. [76]) could be explained in terms of this model. The activity of foreign surface particles should follow that general concept. However, additional effect of the ambient atmosphere must be expected, as confirmed by recent experiments where various solid particles were dusted onto fractured cordierite glass surfaces prior to thermal treatment. The results are summarized in Table 3 [65,66].

Oxide dust particles, having thermal stability, in most cases, were found to provide active nucleating substrates for μ-cordierite. Thus, ZrO_2, known for its thermal stability [78], was found as the most efficient surface nucleation catalyzer. Its nucleating activity was affected by its crystal morphology indicating epitaxial phenomena. In a similar sense, the nucleation activity of dusted μ-cordierite, μ-cordierite, quartz, and fire-clay powders (the latter is a mixture of corundum, μ-cordierite, mullite, and quartz), may be caused by the lattice misfit between these powdered crystals and cordierite crystal. Correspondingly, larger Ns are evident for agate (quartz) ball-milled cordierite glass powders [4], because of the small lattice misfit with cordierite. We note, however, that the stability (and nucleation activity) of oxide particles can be limited by *dissolution* into liquid cordierite. Thus, dusting with TiO_2 and WO_3 reduces N, as is the case of dusting with unstable compounds such as W and WC.

Non-oxide dust particles, having smaller thermal stability, in most cases, did not increase N, except in vacuum ($p < 10^{-4}$ mbar), where better oxidation stability is guaranteed. The inertness of SiC and Si_3N_4 is probably due to the formation of an amorphous SiO_2 surface layer. The increased nucleation activity of these particles under vacuum supports that explanation. In the case of the larger concentrations of unstable particles (W, WC, B_4C or less stable oxides such as WO_3 and B_2O_3), a rippled glass surface (Fig. 20) and the occurrence of foreign crystalline phases were observed,

Table 3
Nucleation activity of solid particles for surface nucleation of μ-cordierite in cordierite glass[a]

Powder	Structure	T_U in °C	Influence on N
ZrO_2 3Y	Monoclinic	2680 (M)	Strong increase
ZrO_2 12Ce	Tetragonal	2680 (M)	
Quartz	Hexagonal	1713 (cristobalite) (M)	
Fire-clay			
μ-Cordierite	Hexagonal	$<\approx$ 1467 (M)	
α-Cordierite	Rhombic	1467 (M)	Increase
Al_2O_3	Trigonal	2050 (M)[(1)]	
Fe_2O_3	Trigonal	1565 (M)	
TiN	Cubic	$< 975(O)$	
TiC	Cubic	$< 975(O)$	
MgO	Cubic	2840 (M)[(1)]	
CeO_2	Cubic	2000 (M)	Slight increase
Si_3N_4 (vacuum)	Hexagonal	≈1900 (D)	
SiC (vacuum)	Cubic	2760 (M)	
WC (vacuum)	Hexagonal	2780 (M)	
B_4C (vacuum)	Rhombic	2450 (M)	
$MgSO_4$	Orthorhombic	1127 (M)	No influence
Si_3N_4	Hexagonal	? (O)[(2)]	
SiC	Cubic	? (O)[(2)]	
K_2SO_4	Orthorhombic	1069 (M)	
WO_3	Rhombic	1473 (M)	Decrease + foreign crystal phases
WC	Hexagonal	$< 975(O)$	
W	Cubic	$< 975(O)$	
TiB_2	Hexagonal	$< 975(O)$	
B_4C	Rhombic	$< 975(O)$	

[a] T_U: expected upper stability limit of the contaminant due to (M) melting, (O) oxidation, (D) decomposition, [(1)] Possibly easy diffusion into the glass), [(2)] amorphous SiO_2 surface layer, see text. Taken from [65].

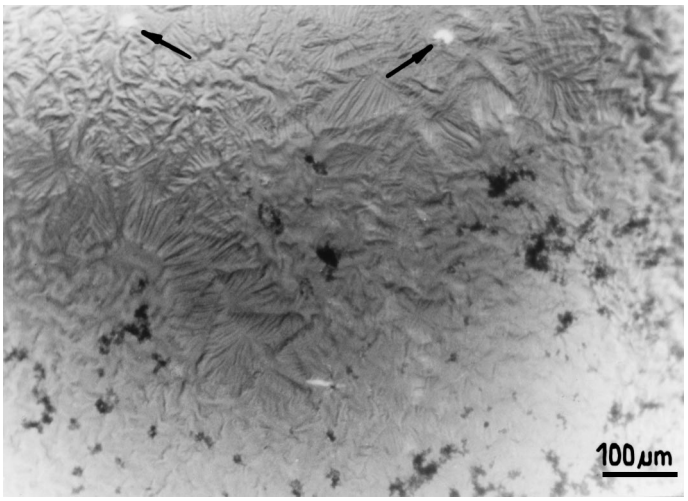

Fig. 20. Fractured cordierite glass surface dusted with W-powder before thermal treatment (15 min, 975°C). Transmission optical micrograph, top view, crossed nicols. Arrows: μ-cordierite crystals. Taken from [61].

indicating chemical interaction with the liquid (dissolution). In the worst case, the latter effect can change the composition of the glass surface layer. Thus, intensive dusting with B_4C triggered crystallization of needle like foreign crystals and caused a rippled surface morphology. These effects can be explained assuming an enriching of B_2O_3 in the near surface area due to oxidation of B_4C and to the well-known decrease of surface tension by B_2O_3 addition [78]. This observation is confirmed by the chemical inertness of B_4C under vacuum. W and WC show similar inertness. Their oxidation is most probably followed by dissolution of the oxide into the melt that modifies the surface morphology. A rippled surface and the total absence of μ-cordierite were also caused by dusting with K_2SO_4. X-ray analysis of a heat-treated mixture of K_2SO_4 and cordierite glass powder showed leucite as the crystal phase [79] indicating dissolution.

Summing up, the nucleating activity of solid *surface* sites is predominantly limited by their chemical stability. Chemical reactions with the glass and with the ambient atmosphere can decrease their nucleating efficiency. Accordingly, all thermally stable furnace tube materials (e.g. fireclay or alumina) turned out, unfortunately, to provide the most active nucleation seeds. The same is true for oxide milling materials [4].

3.3. Ambient conditions

Ambient gases. A strong effect of ambient gases (e.g. water vapor) on surface crystallization was frequently stressed in the older literature. Partridge [56] reported that surface crystallization of $ZnO{\cdot}Al_2O_3{\cdot}SiO_2$ glasses was hindered if the ambient did not contain O_2 or H_2O vapor. Crystal orientation on the surface was affected by heating lithium silicate glass fibers in various atmospheres [80]. However, crystal nucleation was not directly measured. The number of sodium disilicate crystals growing from soda-lime glass surfaces was enhanced in CO_2 atmosphere [22]. Precipitation of sodium carbonate acting as nucleation substrate was proposed as the most likely nucleation mechanism. Frequently, water vapor has been assumed to affect surface nucleation [53,60,81]. However, the nucleation activity of water vapor was claimed to be restricted to temperatures < 375°C [81], $T < 450$°C [60]. Fokin [38] demonstrated an increased N for μ-cordierite at cordierite glass surfaces by repeated wetting and drying. However, N did not correlate with the wetting duration but, instead, with the number of wetting steps and the temperatures of drying.

These observations indicate that heterogeneous surface nucleation is restricted to special sites at the glass surface via condensation or precipitation of reaction products. Thus, the kinetics of nucleation can be controlled by the kinetics of chemical reactions between the glass and the ambient atmosphere, as it might be the case for the data taken from [22] in Fig. 3. In a similar sense, the low nucleation activity of bubble surfaces was often attributed to the presence of precipitates [36] [73]. Hishinuma [82] prevented surface crystallization of $PbO \cdot SiO_2$ glass by means of HF-etching. Correspondingly, the internal surface of amorphous droplets caused by liquid phase separation in $BaO{\cdot}SiO_2$ glasses did not trigger internal heterogeneous nucleation [83].

Recent studies of surface nucleation on cordierite glasses also indicate that *pristine glass surfaces* have no inherent tendency to devitrify. Experiments in glove box conditions did not show any effect of ambient humidity on the surface nucleation density of μ-cordierite, while the crystal growth rate substantially increased with increasing humidity [61]. We should also note that very low N down to $N \approx 10^{-8}$ μm^{-2} ($2l \approx 10$ mm), occasionally occur for freshly fractured surfaces and that such small Ns are typical for fire-polished surfaces, even in air atmosphere (Table 3).

Countless *small surface defects* undoubtedly present at each glass surface (e.g. micro cracks, OH^- groups), evidently do not cause nucleation. In support of this, the number density of OH^- groups at the surface of quartz sand particles is in the range of 10^{-6} μm^{-2} ($2l \approx$ in the nm scale) [84] whereas for (wet) mechanically polished glass surfaces N is between 10^{-1} and 10^{-4} ($2l \approx 3$–100 μm; see Table 2). In a similar sense, a minimum size of active nucleation sites, λ_{min}, is theoretically

predicted [83] and was discussed for heterogeneous volume nucleation on small metal cores [54,85,86] (λ_{min} 8–10 nm; the critical nucleus size at T_g is ≈ 1 nm for silicate glasses [87]). We infer that surface nucleation sites must be much larger than this size. On the other hand, these observations do not exclude the effect of ambient gases or evolved volatiles (e.g. water) on the nucleation activity of special nucleation sites. For instance, the OH-concentration might be increased in the vicinity of surface tips.

Nevertheless, despite the increased molecular mobility at the surface expected from MD calculations [88], *ideally flat* (pristine) glass surfaces should not preferably devitrify due to increased crystal–air interfacial energy, $\sigma_{CA} > \sigma_{CM}$, as stressed in Ref. [75]. This increase can be expected from Eq. (4) because the enthalpy change of evaporation should exceed that of melting. These arguments are supported, for instance, by the well-known effect that surface crystallization of silica glass is triggered by alkaline contamination [96].

Local environment. In addition to the nucleating effect of precipitates caused by chemical reactions of the melt with ambient gases, we expect an additional nucleation effect of airborne dust particles on nucleation. Thus, N was affected by the sample position within the crucible used for the thermal treatment [65,89,90]. N increased at glass surfaces near to a inner crucible wall, while N was decreased by a factor of 2 to 10 for the sample surface that extended out of the crucible into a furnace chamber. Temperature gradients could be excluded due to the uniform crystal size in both samples. Against that background, the effect of neighboring fire-clay or Pt cubes on N was investigated for varied sample-cube-distance, x (Fig. 21) showing a significant increase of N with decreasing x. On the other hand, N was not affected by Pt-cubes. As a speculative explanation, we assume that solid particles, which are more likely emitted from fire-clay and that should probably strike the neighbor glass sample for small x, are responsible for the increase of N.

However, particle bombardment evidently does not increase N at a hot glass surface. Thus, placing a fire-clay block at 1 mm distance to a hot (annealed for 20 min at 950°C) glass sample did not increase N during the second annealing. Accordingly, no bimodal crystal size distribution was evident. These observations might be explained assuming a turbulent air layer that prevents small solid particles from striking the sample surface. Confirming observation was made for cumulative interrupted nucleation treatments of cordierite [91] and anorthite glass [25] were one sample was repeatedly annealed and N was measured. After each annealing step, N increased whereas prolonged one-step annealing of the same total annealing time did not increase N.

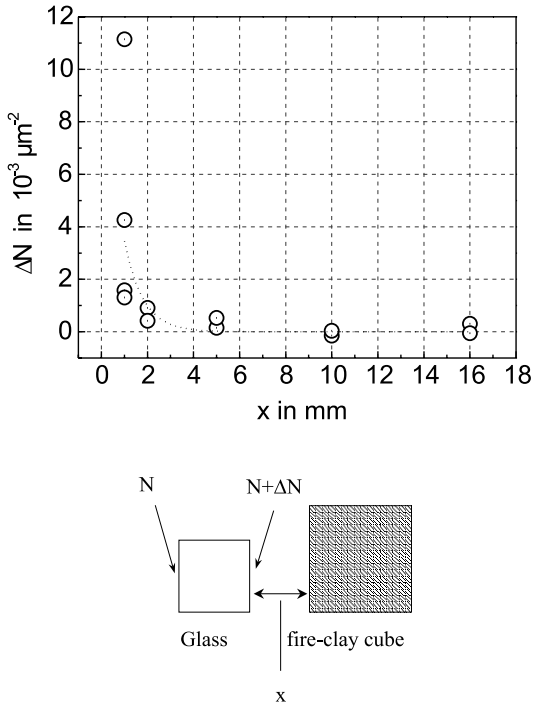

Fig. 21. Effect of the distance x between a polished glass surface and a fireclay cube on N. Taken from [65].

4. Summary

Progress on the general understanding of surface crystallization of glass occurred in the last decade. Despite the fact that the mechanisms of surface nucleation are still not fully understood,

some of the key factors are known and thus it is possible to control the surface nucleation density to a large extent.

Based on improved knowledge concerning the nature of nucleation sites, the surface nucleation density might be utilized as a new technological parameter in the manufacture of both monolithic and sintered glass-ceramics. Further research efforts should include the dominating mechanism triggering surface induced devitrification of multicomponent glasses, the effect of metastable phases and the effect of elastic strains and strain relaxation on the mode of crystallization.

Acknowledgements

Stimulating discussions and advice from the members of the Technical Committee 7 of the ICG: I. Donald, K. Heide, W. Höland, G. Völksch, W. Pannhorst and I. Szabo are deeply appreciated. We also thank Drs E.B. Ferreira and M.O Prado for reviewing the manuscript. E.D.Z. acknowledges the funding provided by CNPq, PRONEX and FAPESP in the period 1985–2000, when most of the surface crystallization studies were performed at the LaMaV/Ufscar. The studies at the BAM were supported by the Schott Glaswerke, FRG, and the Deutsche Forschungsgemeinschaft, which are gratefully acknowledged. R.M. thanks S. Reinsch for his valuable assistance in this study and J. Schmelzer and J. Deubener for their helpful discussions.

References

[1] P.W. McMillan, J. Non-Cryst. Solids 52 (1982) 67.
[2] W. Schreyer, J.F. Schairer, Z. Kristallogr. 116 (1961) 60.
[3] R. Müller, T. Hübert, M. Kirsch, Silikatt. 37 (1986) 111 (Original in German).
[4] R. Müller, S. Reinsch, R. Sojref, M. Gemeinert, Nucleation at cordierite glass powder surface, in: Proceedings of the XVII International Congress on Glass, vol. 5, Bejing, PR China, 1995, pp. 564–569.
[5] R. Müller, Glastech. Ber. Glass Sci. Technol. 67C (1994) 93.
[6] R. Müller, S. Reinsch, R. Sojref, M. Gemeinert, Sintered cordierite glass-ceramics of stoichiometric composition, in: Proceedings of the XVIII International Congress on Glass, American Ceramic Society, San Francisco, 1998 (ISBN I-57498-053-X, order code G042).
[7] I. Gutzow, Contemp. Phys. 21 (1980) 121–137 and 243–263.
[8] I. Gutzow, J. Schmelzer, The Vitreous State, Thermodynamics, Structure, Rheology, and Crystallization, Springer, Berlin, 1995, (ISBN 3-540-59087-0).
[9] P.F. James, J. Non-Cryst. Solids 73 (1985) 517.
[10] I. Gutzow, D. Kaschiev, I. Avramov, J. Non-Cryst. Solids 73 (1995) 477.
[11] D. Turnbull, J. Appl. Phys. 21 (1950) 1022.
[12] S. Manrich, E. Hage, E.D. Zanotto, Aplicabilidade da teoria clássica de nucleação modificada (CD-CNT) à cristalização de polímeros, Polímeros: Ciência e Tecnologia, Janeiro (l992) 15–20.
[13] J.B. Zeldovich, J. Exp. Theor. Phys. 18 (1943) 1.
[14] R. Pascova, I. Penkov, I. Gutzow, in: Proceedings of the 16th International Congress on Glass, Madrid, Bol. Soc. Esp. Ceram. Vid. 2 (1992) 189.
[15] R. Müller, R. Naumann, S. Reinsch, Thermochim. Acta 280&281 (1996) 1919.
[16] E.D. Zanotto, J. Non-Cryst. Solids 219 (1997) 42.
[17] D.G. Burnett, R.W. Douglas, Phys. Chem. Glasses 12 (1971) 117.
[18] Z. Strnad, R.W. Douglas, Phys. Chem. Glasses 14 (1973) 33.
[19] S. Toschev, I. Gutzow, Kristall und Technik 7 (1972) 43.
[20] N.S. Yuritsin, V.M. Fokin, A.M. Kalinina, V.N. Filipovich, Kinetics of crystal nucleation on the surface of cordierite glass, in: Proceedings of the XVI International Congress on Glass, vol. 5, Madrid, 1992, p. 21.
[21] N.S. Yuritsin, V.M. Fokin, A.M. Kalinina, V.N. Filipovich, Ceram. Trans. 30 (1993) 379.
[22] K. Takahashi, T. Sakaino, Bull. Tokyo Inst. Technol. 104 (1971) 1.
[23] N.S. Yuritsin, V.M. Fokin, A.M. Kalinina, V.N. Filipovitch, Glass Phys. Chem. 20 (1994) 116.
[24] N.S. Yuritsin, V.M. Fokin, A.M. Kalinina, V.N. Filipovitch, Glass Phys. Chem. 20 (1994) 125.
[25] E. Wittmann, E.D. Zanotto, J. Non-Cryst. Solids 127 (2000) 94.
[26] N.S. Yuritsin, V.M. Fokin, A.M. Kalinina, V.M. Filipovich, Nucleation and growth of crystals at the surface of glass of the composition $2MgO–2Al_2O_3–5SiO_2$, in: Proceedings of the National Conference on Glassy State, Leningrad, 1986, pp. 235–236.
[27] V. Filipovich, V. Fokin, N. Yuritsin, A. Kalinina, Thermochim. Acta 280&281 (1996) 205.
[28] N. Diaz-Mora, E.D. Zanotto, E.C. Ziemath, Phys. Chem. Glasses 37 (1996) 258.
[29] J. Deubener, R. Brückner, H. Hessenkemper, Glastechn. Ber. 65 (1992) 256.
[30] N.P. Bansal, R.H. Doremus, Commun. Am. Ceram. Soc. (1983) C-132.
[31] E.D. Zanotto, R. Basso, Cristalização superficial em vidros-mecanismos, Cerâmica (São Paulo) 32 (1986) 117–120, 197.

[32] E.D. Zanotto, J. Non-Cryst. Solids 130 (1991) 217.
[33] R. Müller, D. Thamm, Surface-induced nucleation of cordierite glass, in: Proceedings of the Fourth International Otto-Schott-Coll., Jena, Wiss. Beitr. der Friedrich-Schiller-Universität Jena, 1990, p. 86.
[34] R. Müller, S. Reinsch, W. Pannhorst, Glastech. Ber. Glass Sci. Technol. 69 (1996) 11.
[35] E.D. Zanotto, Surface crystallization kinetics in soda-lime-silica glasses, in: Proceedings of the Fourth Otto Schott Coll., Jena 1990, pp. 268–281.
[36] E.D. Zanotto, J. Non-Cryst. Solids 129 (1991) 183.
[37] U. Köster, Mater. Sci. Eng. 97 (1988) 233.
[38] V.M. Fokin, N.S. Yuritsyn, A.M. Kalinina, V.N. Filipovitch, D.N. Filipova, Glass Sci. Technol. 67C (1994) 392.
[39] V.M. Fokin, E.D. Zanotto, J. Non-Cryst. Solids 246 (1999) 115.
[40] E.D. Zanotto, J. Non-Cryst. Solids 89 (1987) 361.
[41] E.D. Zanotto, M.C. Weinberg, Phys. Chem. Glasses 30 (1988) 186.
[42] P.F. James, Adv. Ceram. 4 (1982) 1.
[43] M.J. Davis, P.D. Ihinger, Am. Min. 83 (1998) 1008.
[44] M.J. Davis, P.D. Ihinger, A.C. Lasaga, J. Non-Cryst. Solids 219 (1997) 62.
[45] P.W. McMillan, Glass Ceramics, Academic press, New York, 1964.
[46] A. Dobreva, I. Gutzow, J. Non-Cryst. Solids 162 (1993) 1.
[47] J. Schmelzer, R. Pascova, J. Möller, I. Gutzow, J. Non-Cryst. Solids 162 (1993) 26.
[48] B. Durschang, G. Carl, C. Rüssel, E. Meier-Katzschmann, J.-D. Schnapp, Structure and properties of anisotropic glass-ceramic produced by extrusion, in: Proceedings of the XVII International Congress on Glass, vol. 5, Chinese Ceramic Society, 1995, pp. 216–221.
[49] K. Tabata, J. Am. Ceram. Soc. 10 (1927) 6.
[50] G.W. Morey, J. Am. Ceram. Soc. 13 (1930) 683.
[51] H.R. Swift, J. Am. Ceram. Soc. 30 (1947) 165.
[52] D.M. Mattox, J. Am. Ceram. Soc. 50 (1967) 683.
[53] G. Müller, Fortschr. Miner. 58 (1980) 68.
[54] R.D. Maurer, J. Chem. Phys. 31 (1959) 444.
[55] T. Seidel, C. Friedrich, J. Mater. Sci. 27 (1992) 263.
[56] G. Partridge, P.W. McMillan, Glass Technol. 15 (1974) 127.
[57] G. Partridge, Glass Technol. 28 (1987) 9.
[58] Y. Ding, A. Osaka, Y. Miura, J. Am. Ceram. Soc. 77 (1994) 749.
[59] G. Morgensen, N.H. Christensen, Phys. Chem. Glasses 22 (1981) 17.
[60] F.M. Ernsberger, Phys. Chem. Glasses 22 (1981) 511.
[61] R. Müller, S. Reinsch, G. Völksch, K. Heide, Ber. Bunsenges. Phys. Chem. 100 (1996) 1438.
[62] R. Müller, S. Reinsch, W. Pannhorst, Nucleation at cordierite glass surfaces: Chemical Communications of the Bulgarian Academic Science, in: Proceedings of the 11th Conference on Glass and Ceramics, Varna, 1993, pp. 63–68.
[63] J. Schmelzer, J. Möller, I. Gutzow, R. Pascova, R. Müller, W. Pannhorst, J. Non-Cryst. Solids 183 (1995) 215.
[64] S. Reinsch, R. Müller, W. Pannhorst, Glastech. Ber. Glass Sci. Technol. 67C (1994) 432.
[65] S. Reinsch, R. Müller, G. Völksch, K. Heide, Nucleation sites at silicate glass surfaces, in: Proceedings of the Fifth ESG Conference on Glass Science and Technology, Prag, 1999 (ISBN 80-238-3861-X).
[66] S. Reinsch, R. Müller, Nucleation at silicate glass surfaces, in: Analysis of the Composition and Structure of Glass and Glass Ceramics, Schott Series on Glass and Glass Ceramics, Science, Technology, and Appplication, Springer, Berlin, 1999, p. 372.
[67] R. Müller, D. Thamm, W. Pannhorst, Bol. Soc. Esp. Ceram. Vid. 31-C (5) (1992) 105.
[68] P. Altanzog, R. Müller, S. Reinsch, J. Schmelzer, Glastechn. Ber. Glass Sci. Technol. 71C (1998) 428.
[69] J. Deubener, private communication.
[70] R. de Réaumur, Mém. Acad. R. Sci. (1739) 370.
[71] E.M. Rabinovich, Ceram. Bull. 58 (1979) 595.
[72] J.E. Neely, F.M. Ernsberger, J. Am. Ceram. Soc. 49 (1966) 396.
[73] C.G. Bergeron, J.P. de Luca, J. Am. Ceram. Soc. 50 (1967) 116.
[74] C. Klingsberg, J. Am. Ceram. Soc. 47 (1964) 97.
[75] D.R. Uhlmann, Mater. Sci. Res. 4 (1969) 172.
[76] I. Gutzow, Glastechn. Ber. 46 (1973) 219.
[77] I. Gutzow, I. Penkov, Wiss. Z. Friedrich-Schiller-Unv. Naturwiss. R. 36 (1987) 907.
[78] H. Scholze, Glas. Natur, Struktur und Eigenschaften, Springer, Berlin, 1977.
[79] M. Gemeinert, private communication, 1998.
[80] C.L. Booth, G.E. Rindone, Surface nucleation of glass fibers, in: Proceedings of the VI International Congress on Glass, Washington, 1962, pp. 42–43.
[81] W.D. Scott, J.A. Pask, J. Am. Ceram. Soc. 44 (1961) 181.
[82] A. Hishinuma, MSc Dissertation, MIT, USA, 1986 (cited in /33/).
[83] A.F. Craievich, E.E. Zanotto, P.F. James, Bull. Min. 106 (1983) 169.
[84] L. Kolb et al., in: Oberflächenchemie fester Körper, Wiss. Beitr. d. Friedrich-Schiller-Univers, Jena, 1985, pp. 72–84.
[85] N.H. Fletcher, J. Chem. Phys. 29 (1958) 572.
[86] I. Gutzow, S. Toschev, M. Marinov, E. Popov, Krist. Technol. 3 (1968) 337.
[87] P.F. James, Volume Nucleation in Silicate Glasses in Glasses and Glass-Ceramics, Chapman and Hill, 1989 (ISBN 0-142-27690-9).
[88] A.V. Cardoso, MSc dissertation, Federal University of Minas Gerais, 1988.
[89] G. Völksch, K. Heide, Nucleation in cordierite glasses in dependence on the volatile content, in: Proceedings of the XVIIth International Congress on Glass, vol. 5, Beijing, 1995, pp. 570–575.
[90] G. Völksch, K. Heide, J. Non-Cryst. Solids 219 (1997) 119.
[91] R. Müller, D. Thamm, unpublished results, 1992.
[92] M. Yamane, W. Park, Investigation on the Effect of Surface Condition on the Nucleation and Crystallization of the Glass of Cordierite System, Bericht TC7, 1990.

[93] R. Müller, J. Non-Cryst. Solids 219 (1997) 110.
[94] Y. Bottinga, P. Richet, Earth Planetary Sci. Lett. 67 (1984) 415.
[95] A.M. Kalinina, V.M. Fokin, V.N. Filipovich, Glass Phys. Chem. 12 (1986) 480.
[96] W.C. Heraeus, Z. Elektrochem. 9 (1903) 847.